

Interaction Between the Trapped Electrons and Magnetic Field Gradient and Curvature-Driven Drift Waves in the Toroidal Plasmas

WANG Aike, SANUKI Heiji¹, DONG Jiaqi, ZONCA Fulvio² and ITOH Kimitaka¹

Southwestern Institute of Physics, P.O.Box 432, Chengdu 610041, P.R.China

¹*National Institute for Fusion Science, Toki 509-5292, Japan*

²*ENEA C.R.Frascati, C.P. 65, 00044 Frascati, Rome, Italy*

(Received: 9 December 2003 / Accepted: 12 March 2004)

Abstract

In this paper, we study the interaction between trapped electrons and magnetic field gradient and curvature (MFGC) –driven drift waves. In addition to the MFGC instabilities of long wavelength, a new unstable branch of short wavelength is excited after the trapped electrons are included. It is found that there exist heat pinches in the long wavelength regime. Especially in the position of parallel wave number $k_{\parallel} \approx 0$, the electron-wave resonance strongly destabilizes the modes with the short wavelength, which contribute the significant positive value to ion and electron thermal diffusivities (χ_i and χ_e) but the significant negative value to particle diffusivity (D_e). Finally, a set of nonlinear equations for the MFGC mode with the trapped electron effects is derived and qualitative discussions on it are made.

Keywords:

magnetic field gradient and curvature, trapped electron, drift wave

1. Introduction

It has been realized that the turbulence in plasma is a multiple-length-scale structure [1]. In addition to the long wavelength turbulence, it has been an interesting subject to explore the short wavelength one [2]. Recently, it becomes especially attractive to study the interaction between the different length scale structures [1,3]. Thus, it is desired to obtain a turbulence structure from zero to infinity wave number.

In the previous work [4], we have presented a new kind of instability in the toroidal plasmas: magnetic field gradient and curvature (MFGC)-driven one. The MFGC instability is the long wavelength dominant one. It possesses the finite growth rate even if the plasma pressure gradient vanishes. In addition, no matter what magnitude the plasma pressure gradient is, the instability can be stabilized as long as the magnetic field gradient and curvature is zero.

In this work, we study the interaction between MFGC modes and trapped electrons. In addition to the MFGC instability of long wavelength, a new unstable branch of short wavelength is excited after the trapped electrons are included. Thus, there exist the multi-mode interactions, e.g., those between the two unstable branches and between the stable and unstable branches. As a result, they lead to the present hybrid instabilities with the wave number spectrum of growth

rate from zero to infinity. Subsequently, the effects of the electron-wave resonance on the instabilities and associated transport are emphasized. Finally, a set of nonlinear equations is derived and qualitative analyses on the predicted nonlinear processes are made, which indicate that the nonlinear processes would lead to the minimum energy states satisfying $k_{\parallel} \approx 0$ with the minimum safety factor and turbulent transport level.

2. Linear instability and associated transport

To study the effects of trapped electrons on the MFGC modes, we use two-fluid description in the sheared coordinate system $\hat{e}_{\perp} = \hat{b} \times \hat{r}$ [5], where \hat{r} is radial unit vector and $\hat{b} = \mathbf{B}/B$ is the unit vector along magnetic field \mathbf{B} . Then, the electron response is taken as

$$n_e = n_{e0} [1 + e\phi / T_e + i\delta_{et} e\phi / T_e], \quad (1a)$$

where T_e and n_e are the temperature and density of electrons, respectively, $-e$ is electron charge, and ϕ is electrostatic potential. For the collisionless electron-wave resonance [6]

$$\delta_{et} = \delta_0 k_{\perp} \rho [b_i - \eta_e / 2], \quad (1b)$$

where $\delta_0 = (\pi m_e / 2 m_i)^{1/2} / k_{\parallel} L_n$, $\rho = (T_e m_i)^{1/2} / eB$, $b_i = (k_{\perp}^2 +$

$k_r^2 \rho^2$, and $\eta_e = L_n/L_{T_e}$. Similarly, we have $\eta_i = L_n/L_{T_i}$. Here m_i and m_e are ion and electron mass, and k_\perp and k_r are the perpendicular and radial wave number, respectively; $L_n = -n_e(\partial n_e/\partial r)^{-1}$, $L_{T_j} = -T_j(\partial T_j/\partial r)^{-1}$, and the subscript $j = i, e$ denotes ion and electron species, respectively. Then, following the previous route [4], we obtain the dispersion equation,

$$[b_i \Omega - (1 + i\delta_{et})(\omega_J - \omega_{*p_i} + \omega_{*p_e})] + \omega_{D_i} \Delta_i = \omega_{D_e} \Delta_e, \quad (2a)$$

$$\Delta_i = \left[\frac{5}{3} b_i \Omega + \frac{5}{3} (1 - \tau^{-1} + i\delta_{et}) \omega_{D_i} + \tau^{-1} \omega_{*p_i} \right] (\Omega + \omega_{*p_i} - \frac{10}{3} \omega_{D_i})^{-1}, \quad (2b)$$

$$\Delta_e = \left[\frac{5}{3} (2 + i\delta_{et}) \omega_{D_e} - \omega_{*p_e} \right] (\Omega + \omega_{*p_e} - \frac{10}{3} \omega_{D_e} + \omega_J)^{-1}. \quad (2c)$$

where, $\tau = T_i/T_e$, $\Omega = (\omega - \mathbf{k} \cdot \mathbf{V}_i)$, \mathbf{V}_i is the equilibrium fluid velocity of ions; $\omega_J = (en_e)^{-1} \mathbf{k} \cdot \mathbf{J} = b_J(\omega_{*p_e} - \omega_{*p_i})$ [5], \mathbf{J} is the current density, and $b_J = (q\varepsilon^{-1} k_{\parallel}/k_\perp) - 1$ with the safety factor q and $\varepsilon = r/R \ll 1$ (r and R are the minor and major radius of plasma, respectively); $\omega_{D_j} = -2k_\perp T_j/eBR$ and $\omega_{*p_j} = (1 + \eta_j)\omega_{*j}$. Here Eq. (2a) is obtained by subtracting the continuity equation of electrons from that of ions with the quasi-neutrality condition and Eqs. (2b) and (2c) come from the energy equation of ions and electrons, respectively.

In order to understand the instability described by Eq. (2), it is necessary to discuss Eq. (2) in the two specific cases. First, if the plasma pressure gradient vanishes, *i.e.*, $L_{T_i}^{-1}$, $L_{T_e}^{-1}$, and L_n^{-1} all are zero, Eq. (2) reduces to [4]

$$b_i \Omega^3 - \frac{5}{3} b_i (2 - \tau) \Omega^2 - \left[\frac{5(1 - \tau)\tau + 10}{3} + \frac{50b_i\tau}{9} \right] \Omega - \frac{50}{9} \tau(\tau + 1) = 0, \quad (3)$$

where Ω is normalized to ω_{D_e} . Eq. (3) has generally the unstable solutions. The instabilities are driven completely by the magnetic field gradient and curvature. The MFGC instabilities are the long wavelength-dominated ones due to the finite Larmor radius effect $1/b_i$. The previous fluid models [7] for toroidal ion temperature gradient / trapped electron modes (ITG/TEMs) have no unstable MFGC solutions in the electrostatic case when the plasma pressure gradient vanishes, even if the bad curvature enhances the ITG/TEM instabilities. Compared with those model equations, the present include both the equilibrium fluid velocity of ions and electrons and the continuity and energy equation of electrons. Furthermore, if the magnetic field gradient and curvature is zero, *i.e.*, $\omega_{D_i} = \omega_{D_e} = 0$, from Eq. (2) we have the following unstable solution for Ω :

$$b_i \Omega = (1 + i\delta_{et})(\omega_J + \omega_{*p_e} - \omega_{*p_i}). \quad (4)$$

The instabilities originate in the coupling between the trapped electron effects δ_{et} and the plasma total pressure gradient $L_p^{-1} = -P^{-1} dP/dr \propto (\omega_J + \omega_{*p_e} - \omega_{*p_i})$, which are similar to

the trapped electron-ion temperature gradient modes [7] from the viewpoint of drive sources. Considering Eq. (1b), along with $\omega_J = (en_e)^{-1} \mathbf{k} \cdot \mathbf{J} = b_J(\omega_{*p_e} - \omega_{*p_i})$, we find the growth rate of unstable modes, described by Eq. (4), are direct proportional to the safety factor q , *i.e.*,

$$\gamma = q\varepsilon^{-1} \delta_0 (1 - \eta_e / 2b_i) k_{\parallel} \rho (\omega_{*p_e} - \omega_{*p_i}). \quad (5)$$

Obviously, the instability is the short wavelength dominant one: the larger the wave number, the larger the growth rate. For the short wavelength limit $\eta_e/2b_i$ in Eq. (5) can be omitted.

In the general case with both the finite plasma pressure gradient and the magnetic field gradient and curvature, there exist the interaction between the two unstable branches (3) and (4) and the coupling of the stable branches with the unstable branches. As a result, they lead to the present hybrid instabilities with the wave number spectrum of growth rate from zero to infinity. In particular, the electron-wave resonance in the position of $k_{\parallel} \approx 0$ strongly enhances the growth rate, as shown in Figs. 1 and 2, where $k_{\parallel} \rho = 10^{-7}$. The first unstable branch (solid line) in Fig. 1 is dominated by Eq. (3) and becomes stable in the short-wave length regime. The second unstable branch (dashed line) in Fig. 1 is mainly determined by Eq. (5) and stable in the long wave length regime. Here it should be pointed out that the fluid description and quasineutrality used here are valid for the first branch but only give a qualitative physical picture for the second branch.

Now, we turn our attention to the ion and electron heat

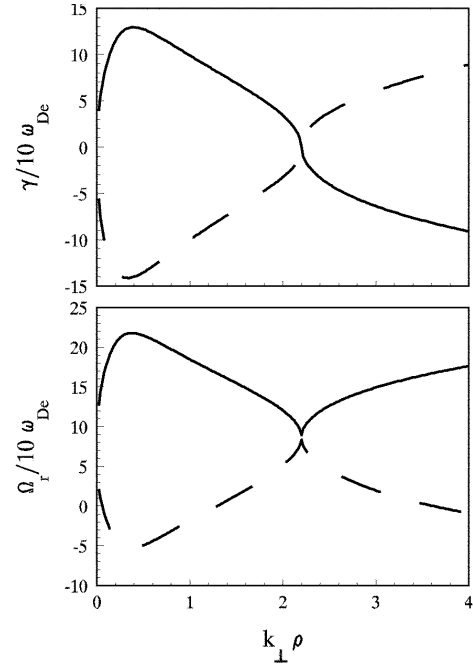


Fig. 1 Growth rate and real frequency for two unstable solutions of Eq. (2a) versus $k_\perp \rho$ (from zero to 4). Solid line is unstable in the regime $k_\perp \rho < 2.2$; dashed line is unstable in the regime $k_\perp \rho > 2.2$ (see, Fig. 2). $R/L_n = 15$, $R/L_{T_i} = 100$, $R/L_{T_e} = 150$, $\tau = 1.5$, $q = 1.5$, $R/\rho = 1500$, and $k_\parallel \rho = 0.4$.

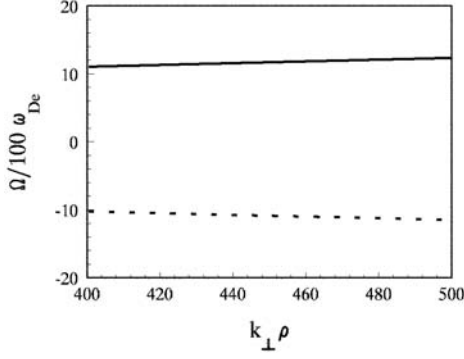


Fig. 2 Growth rate (solid line) and real frequency (dashed line) for unstable short-wave length branch of Eq. (2a) versus $k_{\perp}\rho$ (from 400 to 500). All other parameters are the same as Fig. 1.

and particle transport caused by the hybrid instability. From the definitions of the turbulent fluxes for ion and electron heat and particles, [8]

$$\mathbf{q}_{T_i} = Re\langle \delta T_i \delta \mathbf{v}_{Er}^* \rangle = -\hat{r} \chi_i \partial T_i(r) / \partial r, \quad (6)$$

$$\mathbf{q}_{T_e} = Re\langle \delta T_e \delta \mathbf{v}_{Er}^* \rangle = -\hat{r} \chi_e \partial T_e(r) / \partial r, \quad (7)$$

$$\mathbf{q}_{n_e} = Re\langle \delta n_e \delta \mathbf{v}_{Er}^* \rangle = -\hat{r} D_e \partial n_e(r) / \partial r, \quad (8)$$

along with the assumption for saturated turbulence

$$\tilde{\phi} = 2\gamma / \omega_{D_e} k_r R, \quad (9)$$

we have

$$\mathbf{q}_{T_i} = 2\gamma^3 \frac{5(\tau-1)/3 + 50b_i\tau/9 - (5b_i\tau/3 - 1)(L_n^{-1} + L_{T_i}^{-1})/2}{[\Omega_r - (L_n^{-1} + L_{T_i}^{-1})\tau/2 + 10\tau/3]^2 + \gamma^2} \hat{r} + 2\gamma^2 \delta_{et} \left\{ 1 - \frac{5\tau[\Omega_r - (L_n^{-1} + L_{T_i}^{-1})\tau/2 + 10\tau/3]/3}{[\Omega_r - (L_n^{-1} + L_{T_i}^{-1})\tau/2 + 10\tau/3]^2 + \gamma^2} \right\} \hat{r}, \quad (10)$$

$$\mathbf{q}_{T_e} = \frac{2\gamma^3}{\tau} \frac{[(L_n^{-1} + L_{T_e}^{-1})/2 - 10/3]}{[\Omega_r + \omega_J + (L_n^{-1} + L_{T_e}^{-1})/2 - 10/3]^2 + \gamma^2} \hat{r} + \frac{2\gamma^2}{\tau} \delta_{et} \left\{ 1 + \frac{5[\Omega_r + \omega_J + (L_n^{-1} + L_{T_e}^{-1})/2 - 10/3]/3}{[\Omega_r + \omega_J + (L_n^{-1} + L_{T_e}^{-1})/2 - 10/3]^2 + \gamma^2} \right\} \hat{r}, \quad (11)$$

$$\mathbf{q}_{n_e} = -2\gamma^2 \delta_{et} \hat{r}, \quad (12)$$

where $\delta \mathbf{v}_{Er}$ is the radial fluctuation of $\mathbf{E} \times \mathbf{B}$ velocity, and $\langle \rangle$ refers to a time average. Here both \mathbf{q}_{T_i} and \mathbf{q}_{T_e} are normalized to $T_i R \omega_{D_e} / k_r^2 R^2$, \mathbf{q}_{n_e} to $n_e R \omega_{D_e} / k_r^2 R^2$, the frequencies to ω_{D_e} , and L_n , L_{T_i} , and L_{T_e} to R . Correspondingly, the ion and electron heat and particle transport coefficients, normalized to ω_{D_e} / k_r^2 , are, respectively,

$$\chi_i = \mathbf{q}_{T_i} \cdot \hat{r} L_{T_i}, \quad (13)$$

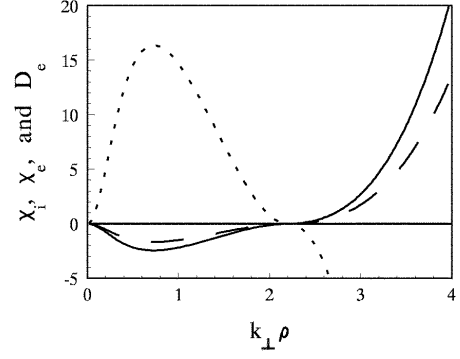


Fig. 3 χ_i (solid line), χ_e (dashed line), and D_e (dotted line) induced by the instabilities in Fig. 1. Here χ_i , χ_e , and D_e are normalized to $10^5 \times \omega_{D_e} / k_r^2$.

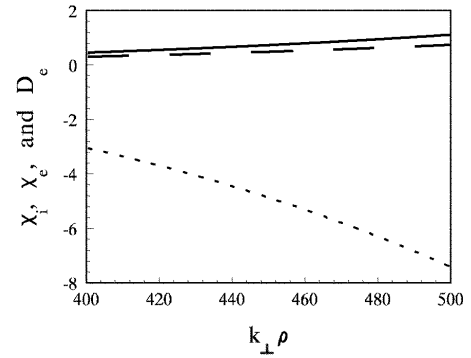


Fig. 4 χ_i (solid line), χ_e (dashed line), and D_e (dotted line) induced by the instabilities in Fig. 2. Here χ_i , χ_e , and D_e are normalized to $10^{16} \times \omega_{D_e} / k_r^2$.

$$\chi_e = \mathbf{q}_{T_e} \cdot \hat{r} \tau L_{T_e}, \quad (14)$$

$$D_e = \mathbf{q}_{n_e} \cdot \hat{r} L_n, \quad (15)$$

where \mathbf{q}_{T_i} , \mathbf{q}_{T_e} , and \mathbf{q}_{n_e} are given by Eqs. (10), (11), and (12), respectively. Here note that, both \mathbf{q}_{T_i} and \mathbf{q}_{T_e} are finite when the plasma pressure gradient vanishes. In the case, the growth rate of instability is given by Eq. (3) and correspondingly, χ_i and χ_e tend to infinite. Furthermore, the transport coefficients χ_i , χ_e , and D_e under the general case with the both finite plasma pressure gradient and the magnetic field gradient and curvature, are shown in Figs. 3 and 4. The present χ_i , χ_e , and D_e in the short wavelength regime ($b_i \gg \eta_e/2$) have the opposite sign with those in the long wavelength regime ($b_i \leq \eta_e/2$). Especially, the electron-wave resonance-excited short wavelength instabilities contribute the significant positive values to χ_i and χ_e but the significant negative value to D_e (particle pinch).

In deriving the above transport coefficients, we used the assumption (9). However, the saturated value for a perturbation, e.g., $\tilde{\phi}$, should be decided by the corresponding nonlinear processes. In the following, we give the nonlinear equations with the interaction between MFGC mode and trapped electrons.

3. Nonlinear modes

In what follows, we use \hat{x} , \hat{y} , and \hat{z} coordinate system, where \hat{x} , \hat{y} , and \hat{z} are counterparts of \hat{r} , \hat{e}_\perp , and \hat{b} in the sheared coordinate system, respectively. Then, we can derive the following set of nonlinear equations

$$k_\perp^2 \frac{\partial \tilde{\phi}_k}{\partial t} + i(1 + i\delta_{et})(\omega_J + \omega_{*p_e} - \omega_{*p_i})\tilde{\phi}_k + i\omega_{D_i}\tilde{p}_{ik} - i\omega_{D_e}\tilde{p}_{ek} - [\tilde{\phi}_k, \nabla_\perp^2 \tilde{\phi}_k] = 0, \quad (16)$$

$$\frac{\partial \tilde{p}_{ik}}{\partial t} + \frac{5}{3}k_\perp^2 \frac{\partial \tilde{\phi}_k}{\partial t} + i \left[\tau^{-1} \left(\frac{5}{3}\omega_{D_i} - \omega_{*p_i} \right) - \frac{5}{3}(1 + i\delta_{et})\omega_{D_i} \right] \tilde{\phi}_k - i(\omega_{*p_i} - \frac{10}{3}\omega_{D_i})\tilde{p}_{ik} + (\tilde{\phi}_k, \tilde{p}_{ik}) - \frac{5}{3}(\tilde{\phi}_k, \nabla_\perp^2 \tilde{\phi}_k) = 0, \quad (17)$$

$$\frac{\partial \tilde{p}_{ek}}{\partial t} - i \left(\omega_J + \omega_{*p_e} - \frac{10}{3}\omega_{D_e} \right) \tilde{p}_{ek} - i \left(\frac{10}{3}\omega_{D_e} - \omega_{*p_e} + i\frac{5}{3}\delta_{et}\omega_{D_e} \right) \tilde{\phi}_k + (\tilde{\phi}_k, \tilde{p}_{ek}) = 0, \quad (18)$$

where the spatial length scale is normalized to ρ , and velocity to $c_s = (T_e/m_i)^{1/2}$; $\tilde{\phi}$, \tilde{p}_i , and \tilde{p}_e are the normalized fluctuations for the electrostatic potential and ion and electron pressure, i.e., $\tilde{\phi} = e\delta\phi/T_e$, $\tilde{p}_e = \delta p_e/P_e$, and $\tilde{p}_i = \delta p_i/P_i$; $[\tilde{\phi}, f] = \delta \mathbf{v}_E \cdot \nabla f$ is the Poisson brackets, and the subscript k expresses the Fourier component of the fluctuation with wave number k . Eqs. (16)-(18) describe the nonlinear processes with interaction between the MFGC modes and trapped electrons, which are retained for the future numerical research. But, qualitative discussion on them is also useful. As we argued previously, the present linear instabilities have the significant growth rates (or energy) in the short wavelength regime, which are direct proportional to the safety factor q (or q^2) and driven by the electron-wave resonance in the position of $k_{||} \approx 0$. Based on the minimum energy principle, we can primarily judge that the nonlinear processes, described by Eqs. (16)-(18), should transfer the energy of the short wavelength modes to the long wavelength modes and meanwhile relax the safety factor q to its minimum (even if the present electrostatic description can not influence q). Consequently, it is possible that $\tilde{\phi}$ in the short wavelength regime is almost in the same order of magnitude as that in the long wavelength regime and thus, the turbulent transports, induced by the different length scale turbulence, approximately cancel each other because the present χ_i , χ_e , and D_e in the short wavelength regime have the opposite sign with those in the long wavelength regime. That is, the wave-wave couplings of nonlinear processes with the electron-wave resonance in the position of $k_{||} \approx 0$ would lead to the minimum energy states satisfying $k_{||} \approx 0$ with the minimum safety factor and turbulent transport level. Such minimum energy states may be candidates to explain the experimental facts that the

transport barriers have been often observed at or near the minimum rational surface.

4. Summary

In this work, we studied the interaction of MFGC modes with trapped electrons. The MFGC instabilities are the long wavelength dominant ones. After the trapped electrons are included, however, a new unstable branch of short wavelength is excited, the growth rate of which is direct proportional to the safety factor q . In the case, there exist multi-mode-interactions, e.g., that between the long and short wavelength unstable branches. As a result, they lead to the present hybrid instabilities with the wave number spectrum of growth rate from zero to infinity. It is found that both χ_i and χ_e is negative (heat pinches) while D_e are positive in the long wavelength regime $k_\perp^2 \rho^2 \leq \eta_e/2$, and inversely, D_e is negative (particle pinch) but χ_i and χ_e are positive in the short wavelength regime $k_\perp^2 \rho^2 \gg \eta_e/2$. In particular, the electron-wave resonance in the position of $k_{||} \approx 0$ strongly destabilizes the modes in the regime $k_\perp^2 \rho^2 \gg \eta_e/2$, which contribute the significant positive values to χ_i and χ_e but significant negative value to D_e .

Finally, we derived a set of nonlinear equations with interaction of MFGC modes with trapped electrons. A qualitative discussion on the corresponding nonlinear processes was made from the linear results and minimum energy principle.

Acknowledgements

This work is supported by the JSPS-CAS Core-University Program on Plasma and Nuclear Fusion, by the Natural Science Foundation of China under Grant Nos. 10375019 and 10135020.

References

- [1] S-I. Itoh and K. Itoh, Plasma. Phys. Controlled Fusion **43**, 1055 (2001).
- [2] A.I. Smolyakov, M. Yagi and Y. Kishimoto, Phys. Rev. Lett. **89**, 125005 (2002).
- [3] Jiquan Li and Y. Kishimoto, Phys. Rev. Lett. **89**, 115002 (2002).
- [4] A.K. Wang, H. Sanuki, J.Q. Dong, F. Zonca, K. Itoh, *Proceeding of the 9th IAEA technical meeting on H mode and transport barriers* (24-26, Sep., 2003, San Diego, USA), contributed paper.
- [5] A.K. Wang, J.Q. Dong, H. Sanuki and K. Itoh, Nucl. Fusion **43**, 579 (2003).
- [6] P.W. Terry and W. Horton, Phys. Fluids **26**, 106 (1983).
- [7] J. Weiland, *Collective Modes in Inhomogeneous Plasma: Kinetic and Advanced Fluid Theory* (2000, Institute of Physics Publishing, Bristol) p115-142.
- [8] M. Fröjd, P. Strand, J. Weiland and J. Christiansen, Plasma Phys. Control. Fusion **38**, 325 (1996).